

CONSTRUCTION OF APPLE II AND IN VACUUM UNDULATORS AT ESRF

J. Chavanne, C. Penel, P. Van Vaerenbergh
 ESRF, B.P. 220 38043 Grenoble Cedex, France

Abstract

Three helical undulators of type APPLE II have been completed and installed in the ESRF storage ring. Their interaction with the stored beam is the result of the usual residual field errors and a predictable horizontal/vertical tune shift which depends on gap and phase. The measured closed orbit distortions and tune shift induced by the ESRF Apple II undulators are presented. The observed tune shift vs. phase is very consistent with expectations. A new shimming technique has been successfully implemented which reduces the tune shift vs. phase. A noticeable improvement of the ESRF performances can be achieved with the use of in-vacuum undulators. Four 2 metres long devices are being fabricated. They have been designed to provide enhanced photon fluxes in the range of 10 to 20 keV (period 17 mm, 18 mm) or at a photon energy above 30 keV (period 21mm, 23 mm). The first results of the field measurements are presented.

1 APPLE II UNDULATORS

APPLE II helical undulators are presently in operation in a number of synchrotron radiation facilities. They have been identified as serious sources of perturbation on the stored electron beam [1], [2]. The interaction of APPLE II undulators with the stored beam is now well understood [5], [6]. It is mostly seen in the usual Closed Orbit Distortion ("COD") and a predictable horizontal/vertical tune shift depending on gap and phase [6]. Due to the complicated magnetic assembly, the field integral correction of APPLE II undulators is difficult, the usual multipole correction based on soft iron shims cannot be easily used [4]. Alternative methods based on magnet block displacements and the use of small magnet block arrays placed at the ends can be used. Assuming sinusoidal horizontal and vertical fields of amplitude $B_{0x}(x,z)$ and $B_{0z}(x,z)$, the tune shifts in both planes are expressed as:

$$dv_{x,z} = \frac{-5.7 \cdot 10^{-4}}{4\pi} \bar{\beta}_{x,z} \left(\frac{\lambda_0}{E} \right)^2 L \frac{\partial^2}{\partial x^2, z^2} (B_{0x}^2 + B_{0z}^2) \quad (1)$$

with λ_0 and L being the period and length of the undulator respectively and $\bar{\beta}_{x,z}$ the average beta function in the horizontal (vertical) plane over the length L. E is the energy of the electrons. The narrow transverse profile of the horizontal field component of APPLE II undulators is responsible for the observation of significant tune shift when the undulator phase is changed at small gaps.

The horizontal tune shift has a strong dependence on the horizontal position making any correction with conventional current-driven quadrupoles difficult. A specific shimming has been developed at the ESRF for this purpose [6].

1.1 Interaction of ESRF APPLE II undulators with the stored beam

Three APPLE II undulators of 1.6 m have been produced and installed on the ESRF ring. Two identical devices of period 88 mm (HU88) are installed in the ID8 straight section. The third device of period 38 mm replaces a 85 mm period helical undulator (helios) in the ID12 straight section. Obviously, the two HU88 are expected to produce the most significant interaction with the stored beam. Both devices induce visible CODs in complete agreement with measured field integrals (figure 1). The larger effect is recorded at the minimum gap when the phase is changed. For both devices there is a residual horizontal field integral variation difficult to correct independently of the vertical component. The complete correction of both undulators has been carried out using steerers placed on each side of the straight section. For the HU38 device, the field integral components remain lower than 10 G.cm at any gap/phase setting.

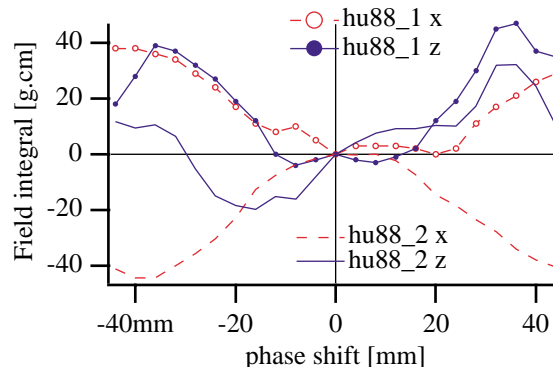


Figure 1: Measured field integral in both planes for the 2 HU88 devices versus phase shift at a gap of 16 mm.

Because of the large K value (4.5) at the minimum gap of 16 mm and the large horizontal beta function (35 m), both HU88 devices were expected to produce visible tune shifts when the phase changed from 0 (taken as a reference) up to 44 mm (horizontal field). Using the 3D magnetic calculations from RADIA together with equation (1) the resulting horizontal tune shift can be

predicted. The agreement between calculated and measured tune shift versus HU88 phase is excellent (figure 2). The measurement of the horizontal tune shift between undulator phase of 0 and 44 mm versus horizontal position has been done using horizontal bumps applied locally on the electron beam. The observed strong dependence versus horizontal position is also in very good agreement with predictions (figure 3). The dedicated “tune shift shimming” has been successfully tested (figure 1). A set of four shims of 0.1 mm thickness was used which improve the tune shift versus undulator phase.

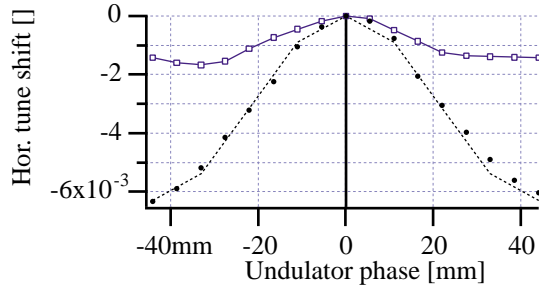


Figure 2: Horizontal tune shift induced on electron beam by a HU88 as a function of undulator phase (gap 16 mm). Dashed line: prediction, black dots: measured values, square dots: measured tune shift with correction shims.

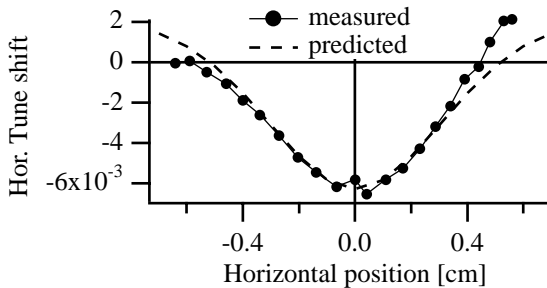


Figure 3: Horizontal tune shift induced by a HU88 as a function of horizontal position (mid-plane of the undulator). Each point corresponding to a variation between an undulator phase of 0 and 44 mm. Black dots: measured values, dashed line: calculated values.

2 IN VACUUM UNDULATORS

Four in-vacuum undulators are presently being produced at the ESRF. All four devices are 2 metres long. The periods have been optimised to enhance photon fluxes at almost fixed energy within 13 Kev (period 17 mm and 18 mm, $K \approx 1$) or above 30 keV (period 23 mm and 21 mm, $K > 1.5$). They are designed to operate at a minimum gap of 6 mm without any reduction of the beam lifetime [7].

2-1 Technology

The support structure is essentially derived from the 1.6 m prototype installed on the ESRF ring since the end of 1999. It is presented on figure 4. Apart from the resulting modification due to the increase in length, the main improvements of the support have been focused on a better heat evacuation within the flexible transitions at

either ends of the magnet assembly (figure 5) and the mechanical connection between the magnetic assembly and the external movable girders. The magnetic assemblies are based on $\text{Sm}_2\text{Co}_{17}$ material, a choice essentially motivated by the required baking temperature (140-150 deg C) and potential radiation damages (continuous or accidental electron beam scraping at low gaps).

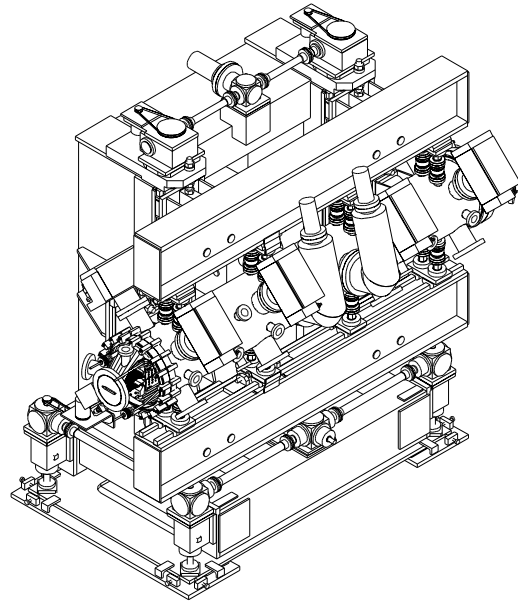


Figure 4: 3D view of the 2 metres long in vacuum undulators

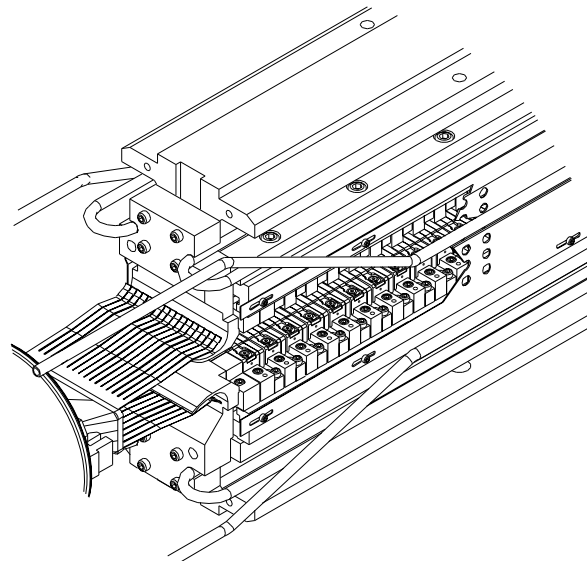


Figure 5. End structure of in-vacuum undulator.

2.2 Magnetic measurements

The magnet assembly consists in very short modules of 1 magnet (M1) or 3 magnets (M3). Each module has been characterized using fast on-the-fly flip coil scans to obtain field integral values versus the transverse horizontal position (41 points every 2.5 mm at 3 mm above magnet surface). Despite the required effort to measure all

modules of an undulator (400 to 500 units) the resulting data proved to be very useful to limit any consecutive multipole shimming. Following the addition of one period (1 module of type M1 and 1 module of type M3) in the assembly the field integral has been controlled using fast on-the-fly scans and the next pair of modules was then selected by software to minimize the r.m.s. value of the field integral versus horizontal position. The end field terminations consist of specific modules (4 magnets blocks) which keep a negligible field integral variation versus undulator gap [3]. The first device has now been completed (period 23 mm). The potential use of high harmonics (>7) in the spectrum of such an undulator required a dedicated spectrum shimming based on vertical displacement (± 0.1 mm) of individual modules. Figure 6 shows the field integral components versus horizontal position at the magnetic axis for a gap of 6 mm. The observed small variations ensure that any residual higher integrated multipoles are negligible. The final on axis field integral dependence versus gap is shown in figure 7, both field integral components being below 10 G.cm at any magnetic gap.

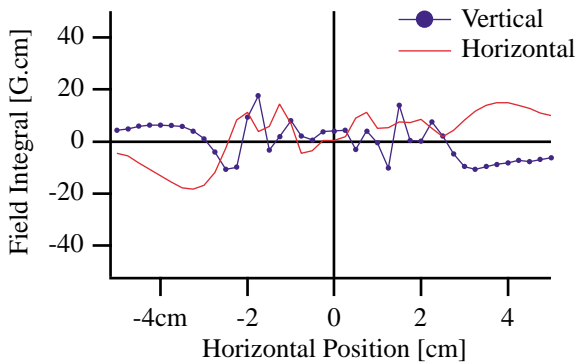


Figure 6: Field integral components of the U23 undulator as a function of horizontal position at a gap of 6 mm.

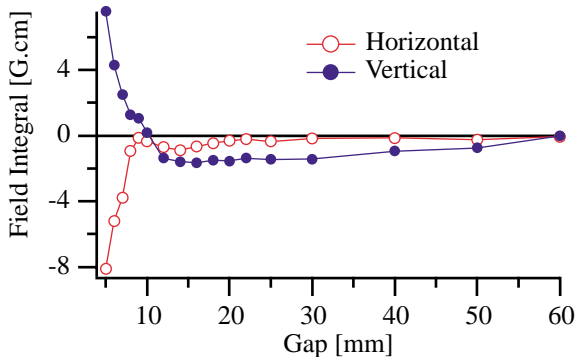


Figure 7: Variation of on-axis first field integral versus U23 undulator gap.

The r.m.s. optical phase error computed at all poles is presented on figure 8. The phase error has been especially minimized at small gaps where the high harmonics of the X-ray spectrum are of practical use. The resulting spectrum computed from a filament mono energetic electron beam (6 GeV, 0.2 A) using field measurement is

compared to an ideal spectrum produced by an error-free undulator (pure sinusoidal magnetic field) in figure 9.

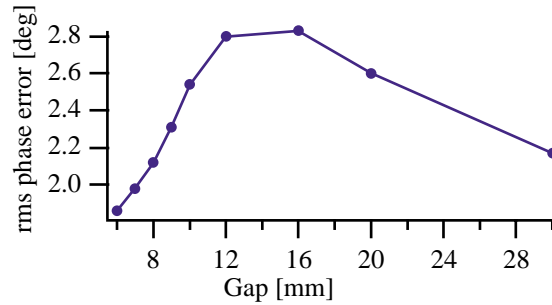


Figure 8: r.m.s optical phase error as a function of gap for the U23 undulator.

At a gap of 6 mm, the r.m.s. phase error was initially 4.5 degrees, it has been reduced to below 2 degrees after the spectrum shimming. This illustrates the feasibility of this method for very small gap and short period undulators. The magnetic measurement of the three other undulators (U17, U18 and U21) has just started.

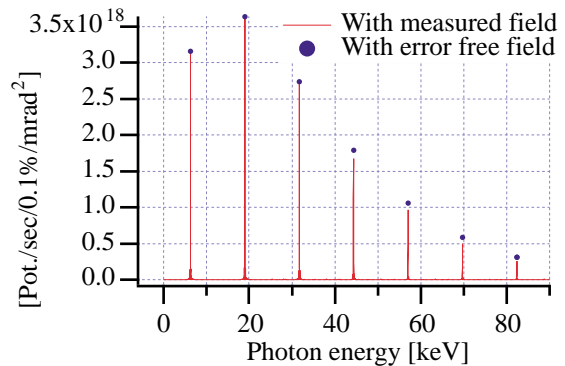


Figure 9: Calculated spectrum from a filament electron beam ($E=6$ GeV, $I=0.2$ A) for the U23 undulator at a gap of 6 mm. Continuous line: actual undulator, dots: ideal error-free undulator.

3 ACKNOWLEDGEMENTS

The authors thank B.Plan from the drafting office for the supervision of all mechanical designs, and R. Kersevan, M. Hahn for their support on all vacuum related activities.

4 REFERENCES

- [1] L.Tosi et al., EPAC 2000 , p2349-1351
- [2] C. Steier et al., EPAC 2000, p2343-2351
- [3] J. Chavanne et al., PAC 99, p 2665-2667
- [4] B. Diviacco et al., PAC 99,p2680-2681
- [5] P. Elleaume , Rev.Sci.Inst.,(15-19 July 1991),p321
- [6] J.Chavanne et al., EPAC 2000, p2346-2348
- [7] J.Chavanne et al, PAC 99, p2662-2664.